Original Article

Synthesis of Bio-Active Silver Nanoparticles against Human Lung Cancer Cell Line (A549) with Little Toxicity to Normal Cell Line (WRL68)

Talib, K. M[1], Oraibi, A. G[2]*, Abass, G. I[3]

1. The Iraqi Ministry of Education, Karkh II Education Directorate, Baghdad, Iraq
2. Department of Plant Biotechnology, College of Biotechnology, Al-Nahrain University, Jadriya, Baghdad, Iraq
3. Iraqi University, College of Education, Baghdad, Iraq

How to cite this article: Talib KM, Oraibi AG, Abass GI. Synthesis of Bio-Active Silver Nanoparticles against Human Lung Cancer Cell Line (A549) with Little Toxicity to Normal Cell Line (WRL68). Archives of Razi Institute. 2023;78(5):1624-37.

DOI: 10.32592/ARI.2023.78.5.1624

Article Info:
Received: 15 January 2023
Accepted: 17 January 2023
Published: 31 October 2023

Corresponding Author's E-Mail:
asma.ghatea@nahrainuniv.edu.iq

ABSTRACT

Nanomaterials are characterized by mechanical, thermal, chemical, biological, and other properties that are different from the basic materials that make them up due to their large surface area to size ratio and quantum effect. There are multiple ways to produce nanomaterials mechanically, chemically, and physically, but they are not safe for the environment. Researchers have sought to find safe methods for the production of nanomaterials, such as green manufacturing, that is, manufacturing nanomaterials from plants. Moreover, there are other sources, such as bacteria or fungi that are used in the production of nanomaterials. This study aimed to try to find an alternative to chemically manufactured drugs, such as those used in the treatment of human cancers, through nanotechnology and from plant sources (green-biosynthesis), which is characterized by abundance and low economic cost. Silver nanoparticles were green-synthesized using an aqueous extract of the licorice plant, their properties were diagnosed, and their differences with the crude aqueous extract were determined. The sizes of nanoparticles were within the range of 60.27-89.80 nm, while the sizes of the crude aqueous extract particles were within the range of 53.96-113.1 nm. Atomic force microscopy was used to find out the shapes, topography, roughness, and protrusions of the surfaces of biosynthesized AgNPs and aqueous extract particles, where the roughness rate of the nanoparticles was 75.54 nm, while it appeared. *In vitro* test of AgNPs showed a higher anti-lung cancer activity against the A549 cell line than that of the extract at an inhibitory concentration for half of the cells used in the experiment (IC_{50}) of 58.78 µg/ml while the IC_{50} of the extract was 67.44 µg/ml. The results showed that the toxicity of AgNPs on the normal hepatocyte line (WRL68) was less than that of the aqueous extract, with IC_{50} concentrations of 244.2 and 147.0 µg/ml, respectively. It is worth mentioning that the lower IC_{50} led to higher toxicity.

Keywords: A549 cell line or WRL68 cell line, *Glycyrrhiza glabra* L., Licorice plant AgNPs, Silver nanoparticles

1. Introduction

The global passion for nanotechnology has increased recently. The term "Nano" is mainly derived from the Greek word "Nanos", which means dwarf (1). Nanomaterials are characterized by mechanical, thermal, chemical, and biological properties that are different from the basic materials that make them up due to their large surface area to size ratio and quantum effect (2). There are multiple ways to produce nanomaterials mechanically, chemically, and physically, but they are not safe for the environment.

Researchers have sought to find safe methods for the production of nanomaterials, such as green manufacturing, that is, manufacturing nanomaterials from plants. Moreover, there are other sources, such as bacteria or fungi that are used in the production of nanomaterials (3, 4). Since chemical and physical methods are expensive and include many limitations, scientists have developed a clean, economical, and environmental-friendly biological approach as an alternative method for nanomaterials production (5).

Silver nanoparticles are defined as silver metal nanoparticles ranging in size from 1 to 100 nm (6). Nanoparticles are used in many fields, such as medicine, engineering, magnetic fields, energy and environmental treatment, and cosmetics (7, 8). One of the modern applications of nanoparticles is their usage in the detection and treatment of tumors. Lung cancer is one of the most common cancers, and the number one cause of cancer death in the world, with 2.90 million new cases and 1.76 million deaths estimated in 2018, according to the GLOBCAN database. It is advanced and cannot be cured, therefore, it leads to death, which makes it one of the most important challenges and problems facing the world in general and Iraq in particular. In recently published reports, the number of lung cancer cases has reached 2,132 in Iraq (9, 10).

Researchers have devised a technique that facilitates the study of the effect of experimental treatment on various types of cancer cells *in vitro*, and this technique is called tissue culture. Knowing the extent of the toxic effect (Cytotoxic effect) of the materials to be tested. It could control the environmental conditions for the development of cancer cells, such as heat, humidity, and nutrition, and also control the time of treatment. In addition, it is possible to control the number and types of cultured cells to determine the efficiency and the toxic effect of therapeutic substances on transplanted cancer cells (11). Therefore, this study was designed to try to find an alternative to chemically manufactured medications, such as those used in the treatment of human cancers, through nanotechnology from plant sources (green-biosynthesis), which are characterized by abundance and low economic cost.

2. Materials and Methods

2.1. Plant Sample Collection

The licorice plant was collected from the local market in Baghdad, Iraq in September 2021 and its classification was confirmed by the National Herbal Commission/General Commission for Agricultural Research.

2.2. Preparation of the Aqueous Extract of the Licorice Plant

The aqueous extract of the licorice plant was prepared using the traditional method (12) by washing the plant parts with water to remove the contaminants from the surface and drying them well with dry air. In total, 50 g of licorice powder was ground, placed in a 500 ml glass beaker containing 250 ml of deionized water and then the mixture was heated in a water bath at 45 °C for 30 min. Afterward, the extract was filtered using Whatman No. 1 filter paper, and stored at a temperature of 4 °C for later use.

2.3. Preparation of the Silver Nitrate Solution

For the preparation of the concentration of silver nitrate solution (1 mM), the following molarity law was used:

$M=W/(M.wt)\times1000/V$

W: Weight

M.wt: Molecular weight

V: Volume (Liters)

- (1Molar.=1000mM)
- M.wt $AgNO_3$=169.87

- V=100 ml

0.001=W/169.87×1000/100=W= 0.016987 g

At this step, 0.016987 g of silver nitrate was dissolved in 100 ml of deionized water to obtain 1 mM of silver nitrate solution ready for use.

2.4. Biosynthesis of Silver Nanoparticles (Green Manufacturing)

Silver nanoparticles of licorice extract were synthesized according to Al-Othman, El-Aziz (13). For this purpose, 10 ml of aqueous extract of licorice was mixed with 100 ml of 1 mM silver nitrate solution, and the mixture was heated on a magnetic vibrating plate at a temperature of 45 °C for 20 min. Observation of the mixture color change was adopted as preliminary evidence for the construction of silver nanoparticles. Afterward, 100 ml of silver nitrate solution of 1 mmol concentration prepared before was kept for the purpose of adopting it as a control in some measurements.

2.5. Preparation of Different Concentrations of Silver Nanoparticles and Plant Extract

Four different concentrations of each of the licorice aqueous extract and the biosynthesized silver nanoparticles (0.375, 0.75, 1.5, 3.0 mg/ml) were prepared sequentially. The extract and nanoparticles were dried after preparation and the concentrations were kept until use in the following experiments.

2.6. Detection and Characterization of Biosynthesized Silver Nanoparticles

Prepared samples were diagnosed using the following methods:

2.6.1. Field Emission Scanning Electron Microscopy

The French MIRA3 Field Emission Scanning Electron Microscopy (FE-SEM) Scanner was used to determine the shape and size of biosynthesized particles in prepared samples (14) by placing approximately 5 µl of ready-to-examine solutions onto a gold-carbon electron microscope holder clipped. Afterward, there were left at room temperature to dry and were tested using different magnifying powers.

2.6.2. Atomic Force Microscopy

Atomic force microscopy (AFM, Angstrom Advanced AA2000) was used to determine the surface morphology and roughness of the prepared silver nanoparticles as well as their size and diameter. For this purpose, a small drop of the sample solution was placed on a 1×1 cm glass slide and left to dry at room temperature until it was ready to be tested according to Qader, Rashid (15).

2.6.3. X-Ray Diffraction

Biosynthetic silver nanoparticles were centrifuged at 10,000 rpm for 15 min, then re-dispersed in sterile double-distilled water and centrifuged again at 10,000 rpm for 10 min. The biosynthesized nanoparticles were dried at 50 °C in an oven and analyzed by X-ray diffraction (XRD). The XRD measurement of biosynthesized silver nanoparticles was performed by aqueous extract of licorice plant using Cu-Kα radiation source in 20-80 scattering range on a 45 kV device and a current of 40 mA. The presence, crystalline nature, phase diversity, and grain size of silver nanoparticles were determined by XRD spectroscopy (16).

2.6.4. Ultraviolet-Visible Spectrometer

A sample was taken 48 h after the preparation of the green nanoparticles, and it was examined by an ultraviolet-visible spectrometer with a wavelength of 190-1100 nm. Deionized distilled water was used where the optical properties of the product were examined at room temperature (17).

2.7. Tissue culture

2.7.1. Cell Lines Humanity

Cell lines were obtained from the Center for Natural Product Research and Drug Discovery, Department of Pharmacology, Faculty of Medicine, University of Malaya, Kuala Lumpur, Malaysia and Cell Line Development and Testing at the Biotechnology Research Center at Al-Nahrain University, Baghdad, Iraq.

2.7.1.1. A459 Cell Line

Lung cancer cell line, a carcinoma cell line of human lung basal-alveolar epithelial cells, first developed in 1972 and taken from the lung tissue of a 58-year-old

Caucasian man with lung cancer. The A549 cells are used as models to study lung cancer and develop treatments for it (18, 19).

2.7.1.2. WRL68

Normal human fetal hepatocyte line, which is a normal cell line similar in shape to adult hepatocytes and transplanted primary hepatocytes. This cell line has been shown to secrete serum albumin and alpha-fetoprotein (enzymes produced by the liver) (20).

2.7.2. Sterilization Methods in Tissue Culture

2.7.2.1. Moist Heat Sterilization

Sterilization of solutions and some laboratory instruments were performed by autoclaving at 121 ℃ and 15 psi pressure for 15 min.

2.7.2.2. Sterilization by Filtration (Membrane Sterilization)

This method is used to sterilize sensitive solutions using the filtration method (microfiltration with a diameter of 0.22 μm).

2.8. Media, Reagents, and Solutions Used in Tissue Culture

Media, reagents, and solutions were prepared according to Freshney (21).

2.8.1. Phosphate Buffer Saline

This solution was prepared by dissolving 8 g of sodium chloride NaCl, 0.2 g of KCl, and 1.15 g of NaH2PO4 in 800-900 ml of distilled water, with a pH adjusted to 7.2 after it was completed to 1 L, and then placed in an autoclave for sterilization and stored at 4 °C until use.

2.8.2. Trypsin Solution

It was prepared by dissolving 1 g of trypsin powder in 100 ml of Phosphate Buffer Saline (PBS) and sterilizing it by filtration ("0.22 mM/Pur" filter paper). The solution was dispensed into 10 ml tubes and kept at -20°C.

2.8.3. Tetra-Diamine-Ethylene Solution

It was prepared by dissolving 1 g of tetra-diamine-ethylene (EDTA) in 100 ml of PBS. Afterward, it was sterilized in a purifier for 10 min, and the prepared solution was divided into 10 ml tubes and stored at 4 °C.

2.8.4. Trypsin Solution-EDTA

This solution was prepared by mixing 20 mL of trypsin solution, 10 mL of EDTA solution, and 370 mL of PBS buffer. This mixture was stored at 4 °C.

2.8.5. Trypan Blue Stain

This dye was prepared by dissolving 1 g of powdered dye in 100 ml of PBS solution, filtering it using filter paper (Whatman No.1), then storing it at a temperature of 4 °C. The prepared dye must be diluted before use in a ratio of 1:10 of PBS solution according to the stock of the processing company.

The serum-free media used in this study was Roswell Park Memorial Institute (RPMI)-1460 (Ready Food Medium) extracted from fetal bovine serum.

2.9. Detection of the anti-tumor effect of biosynthesized AgNPs and aqueous extract of licorice plant on the human lung cancer cell line (A549) and the extent of cytotoxic effect on the normal liver cell line (WRL68) *in vitro*

2.9.1. Maintenance and Preparation of Cell Lines

Maintainance and preparation of cell lines were performed according to Freshney (21). The A459 and WRL68 cells were individually placed in a water bath at 37 °C in order to thaw. Afterward, the cells were distributed into culture flasks (culture flasks containing RPMI-1640 nutritional media) and allowed to fully diffuse in culture vials for 24 h in a humid atmosphere. Subsequently, they were placed in an incubator containing carbon dioxide (CO2) at a temperature of 37°, and when it was confirmed that there was growth in the cell culture and that it was free from contamination, secondary cultures were conducted to multiply them.

Afterward, the cells were examined with an inverted microscope to ensure their vitality. They were free of contamination and grew to the required number (600-700 cells/ml), meaning that the cells reached 80% confluence. Then the cells were transferred to the growth booth, the growth medium was removed (1640-RPMI), and the adherent cells were washed twice with

PBS solution. Afterward, 2-3 ml of trypsin-EDTA solution was added to the cultured cells and monitored to change from a monolayer to single cells by incubating the flask at 37 °C for 1-2 min until the cells were separated from the surface of the flask. Afterward, the entire activity of trypsin was stopped by adding RPMI-1640 nutrient medium again.

The cells were collected in centrifugal tubes and placed in a centrifuge at 2,000 rpm for 10 min at room temperature to precipitate the cells, remove trypsin and the used culture medium, remove the filtrate, and distribute the cell suspension (cells+medium) to other vials containing RPMI. To obtain the required concentration using the cell-counting method, a specific volume of the cell suspension was taken, the same volume of Trypan Blue dye was added to it, and the cells were counted microscopically.

Total Cell Count mL^{-1}=Cell count×Dilution Factor (Sample Volume)×10^4 (21).

Total cell count: number of cells in 1 ml of solution

Cell count: number of cells in a slide

Dilution factor: the dilution factor (sample size)

10^4: Chip Dimensions

The culture flasks were placed in the incubator containing 5% CO_2 for 24 h at 37 °C to ensure that there is no growth and that the cells are free from contamination.

2.9.2. Detection of the viability of A549 lung cancer cells and WRL68 hepatitis cells after treatment with biosynthesized silver nanoparticles from licorice plant and its aqueous extract by MTTassay Method

The method of Ahmed, Al-Saffar (22) was used in a vitality detection experiment as follows:

2.9.2.1. MTT Kit Contents

- MTT solution 1 ml×10 glass vials
- Solubilization solution 50 ml×2 bottles

2.9.2.2. Protocol

- Cells were grown (1×[10]^6 cells mL-1) and then the cell suspension was placed in a plate containing 96 holes with a flat bottom. The plates were covered with sterile film and gently shaken. The final volume of each hole was 200 µl of culture medium.
- It was incubated in a 5% CO_2 incubator at a temperature of 37 °C for 24 h, and the medium was removed after incubation.
- Add the prepared concentrations of aqueous extract of licorice and biosynthetic silver nanoparticles (25, 50, 100, 200, 400 µg mL^{-1}) to the pits of the plate.
- Three replicates were used for each concentration, including the standard control (cells+medium).
- The plate was incubated for 24 h at 37 °C.
- 10 µl of MTT solution was added to each hole at a concentration of 0.45 mM/mL.
- The plate was incubated for 4 h at 37 °C.
- 100 µl of solubilization solution was added to each hole for 5 min to carefully dissolve the medium.
- The absorbance was measured using an Elisa reader at a wavelength of 575 nm.
- The result of the ELISA reader (optical density OD data) was subjected to statistical analysis to determine the concentration of nanoparticles and aqueous extract (IC_{50}) needed to decrease the growth capacity of each cell line according to the following equation:

Viability (%): (optical density of sample)/(optical density of control)×100%

Viability (%): the percentage of cell viability

Optical density

Sample

Control: standard control

2.10. Statistical and Experimental Design

GraphPad Prism version 9 (Graphpad Software Inc., La Jolla, CA) was used to study the cytotoxic effect of AgNPs on cell lines used in the experiments and compare the significant differences between treatments according to the probability values.

3. Results and Discussion

The results showed the final chromatic appearance of the aqueous extract of licorice plant (*Glycyrrhiza glabra*) powder (Figure 1), which was yellow in color as shown in figure 1. This result is consistent with those of the study performed by Nazari, Rameshrad (23),

who showed that the main reason for the yellow color is the presence of the active compounds of flavonoids in the plant. This result also agreed with those of other studies that included extracts of other types of plants. For instance, Hamady, Mohammed (24) in their study examined plant extracts of mint, lemon, and fish as well as the color of the extracts in the three plants. Moreover, it was in line with the results of a study carried out by Abdullah and Dhahi (25) that dealt with grape seed extract. However, the findings were in contrast with those of a study performed by Qader, Rashid (15), where the aqueous extract of ivy appeared brown.

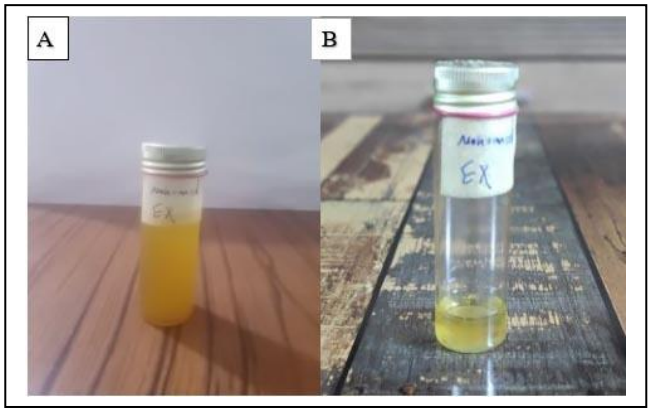

Figure 1. Final color profile of the aqueous extract of licorice (*G. glabra*)
A: Color change after 20 minutes of extraction
B: Color change 24 hours after extraction

The results of biosynthesis of silver nanoparticles from the aqueous extract of the licorice plant (Figure 2) showed the color change of the aqueous extract after the addition of silver nitrate $AgNO_3$ for 20 min while stirring at 45 °C. Accordingly, the color changed from yellow to dark brown, which confirmed the occurrence of an interaction between the active compounds in the plant extract with nitrate salt for the reduction process and the formation of nanoparticles. The color change is a clear initial sign of the formation of silver nanoparticles and positive green biosynthesis. This result is in agreement with those of a study performed by Abdullah and Dhahi (25), who used the seeds of the grape plant and silver nitrate for the biosynthesis of silver nanoparticles.

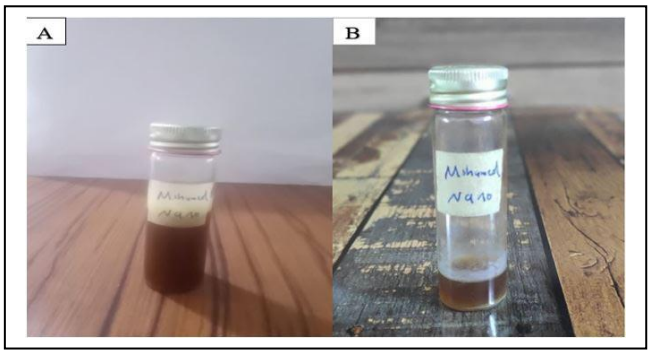

Figure 2. Final color profile of the aqueous extract of licorice (*G. glabra*) after addition of silver nitrate and forming silver nanoparticles
A: The color change 20 minutes after the reaction
B: Color change 24 hours after the reaction

Results in figure 3 illustrate the usage of FE-SEM for biosynthesized silver nanoparticles characterization. Accordingly, the shape and size of the aqueous extract particles appeared lumpy and these particles size ranged from 53.96 nm to 113.1 nm, including oval and irregular spherical shapes. It is worth noting that the colors of some aqueous extracts of different plants look similar to the eye, but when examined with a FeSEM microscope, differences in their sizes and shapes were recorded.

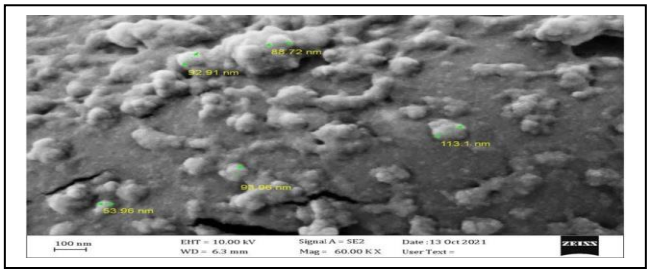

Figure 3. The size and shape of the particles of aqueous extract of licorice powder by FeSEM

This is in line with the results of the research conducted by Qader, Rashid (15), who reported that the color of the water extract particles of ivy plant was yellow and similar to that of the aqueous extract of licorice in the current study. However, when they examined it with a FeSEM microscope, a difference was recorded from the aqueous extract of the licorice

plant. Accordingly, in the aforementioned study, the particles of the extract appeared in a regular rectangular shape and sometimes irregular, and the sizes of the particles ranged from 27,451 nm to 325.49 nm. This was different from the results of the current study.

Figure 4 shows the difference in the shape and size of the manufactured silver nanoparticles from the shape and size of the aqueous extract, as they were spherical and not lumpy. Moreover, the sizes of the nanoparticles were within the range of 60.27-89.80 nm, and these usually were the limits of the sizes of the manufactured nanoparticles (1-100 nm). The limits of this study agreed with the results of previous research, where the sizes of silver nanoparticles, manufactured for a study conducted by Alwaan, Jdyea (28), for celery and myrtle plants ranged from 19.58 nm to 53.16 nm.

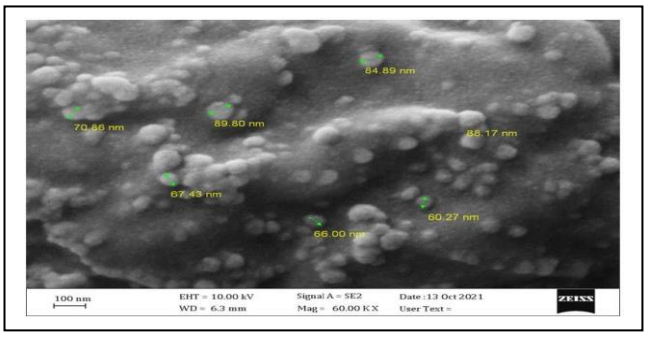

Figure 4. The size and shape of silver nanoparticles manufactured from licorice extract using FeSEM

It also agreed with the study of Hamady, Mohammed (24), who used extracts of fish, lemon, and mint to manufacture silver nanoparticles. The particle sizes in their study ranged from 20.61 nm to 42.90 nm. However, results of the study carried out by Qader, Rashid (15) showed a difference as the sizes of the biosynthetic silver nanoparticles from ivy and aloe vera were within the range of 25.68-141.17 nm and 27.2-109.8 nm, respectively.

Atomic force microscopy makes it possible to know the shapes, topography, roughness, and protrusions of the surfaces of particles and different particles represented by surface heights and surface structure. This technique refers to digital images that allow quantitative measurements of surface features and provides two-dimensional and three-dimensional images and allows their analysis from different directions.

Figure 5 shows that the size of the granules of the aqueous extract of the licorice plant is within the range of 0-20.4 nm at a rate of 8.64 nm. Figure 6 indicated that the surface roughness was 35.97 nm and the value of the mean square root amounted to 4.161. This value was defined as the sum of the surface heights and depressions divided by the sum of their number under the square root. This value is a guide to the roughness of the surface. The maximum cumulative rate of 236 molecules of licorice extract was 14.87 or 55.63%.

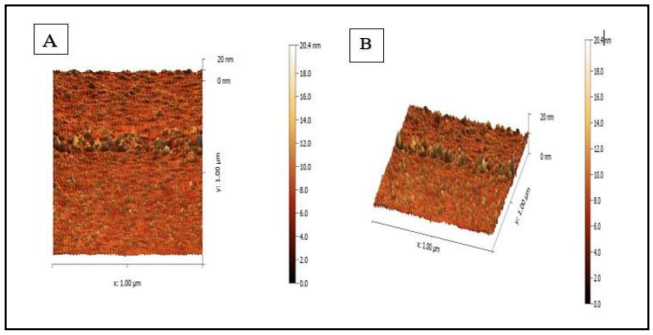

Figure 5. Atomic force microscopy AFM showing the size of the aqueous extract of licorice plant **A:** 2D shape, **B:** 3D shape

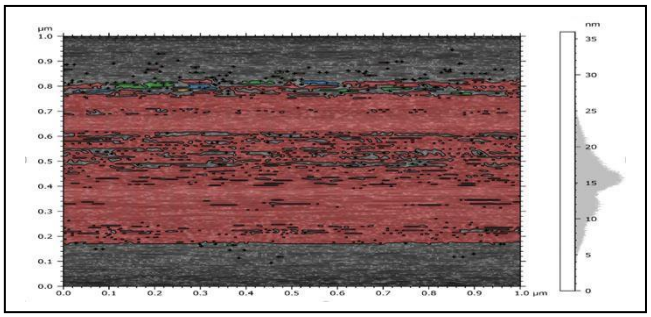

Figure 6. AFM detection for the crude aqueous extract of licorice

Figure 7 shows the data of atomic microscopy for biosynthesized silver nanoparticles that their sizes were within the range of 0-12.7 nm at a rate of 4.96 nm. Figure 8 indicates that the surface roughness and the root mean square value were 75.54 nm and 14.08 nm, respectively. Here, the difference is clear from the characteristics of the

crude water extract, that the biologically manufactured nanoparticles possess a high roughness rate. This indicates an increase in its anti-biological effectiveness, the maximum cumulative rate for 94 manufactured nanoparticles, which amounted to 51.87 and the presence rate of 55.03. The results of the current study were different from those of previous research that dealt with the AFM examination of nanoparticles manufactured from different plants, which indicates the difference in the nature of this examination, compared to other tests. In a study performed by Qader, Rashid (15), it was reported that the sizes of nanoparticles manufactured from ivy and aloe vera plants were 90.07 nm and 53.3 nm, with a roughness of 15.9 nm and 7.67 nm, respectively. Moreover, in a study conducted by Alwaan, Jdyea (28), which dealt with the manufacture of silver nanoparticles from different plants, the average size of nanoparticles was within the range of 17.90-22.97 nm.

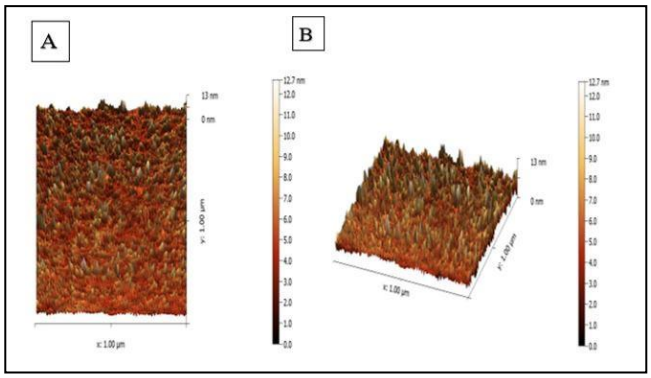

Figure 7. Atomic force microscopy (AFM) detection of silver nanoparticles manufactured from licorice extract
A: 2D shape, **B:** 3D shape

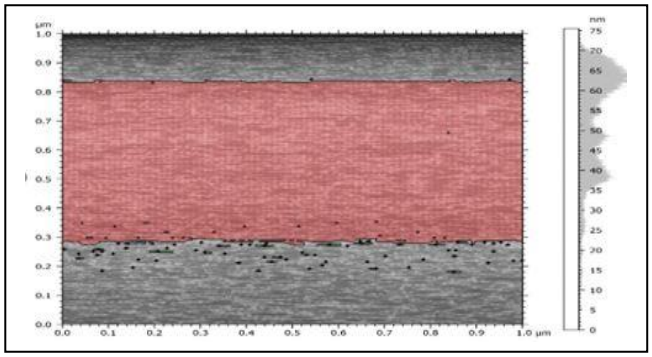

Figure 8. Atomic Force Microscopy (AFM) detection for surface roughness of silver nanoparticles manufactured from licorice extract

The analysis results of the size and crystalline nature of both the crude aqueous extract of licorice plant and the biosynthesized silver nanoparticles using an XRD device showed a clear difference between them. The XRD analysis of the crude aqueous extract showed impurities and irregular clusters, and the emergence of different peaks among strong, medium, and weak, which indicates the presence of several effective compounds in the extract (Figure 9), that many clear peaks measuring 2θ at the angles (26.95°, 31.66°, 38.18°, and 44.92°), the crystalline size of the particles of the crude aqueous extract of licorice plant for the summit, which has a strength of 100% at the angle of 31.66°, using the Debye-Scherrer equation s ($D=0.94\lambda/\beta \cos \theta$), and the average crystalline size of the extract was 14.61 nm.

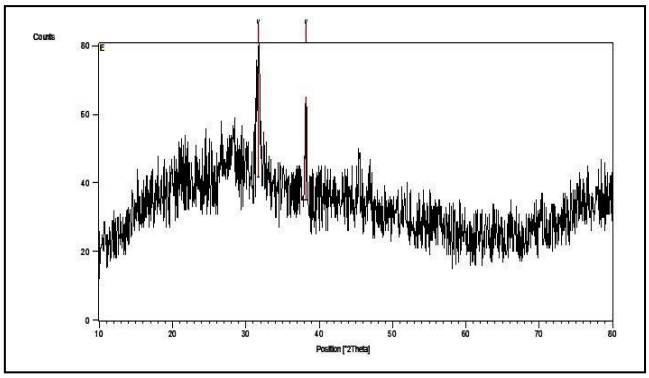

Figure 9. X-ray diffraction of aqueous extract of licorice plant

Figure 10 shows that the nanoparticles appeared in the form of more regular clusters, with few impurities, of high purity. It also shows the presence of a mixture of silver particles and repeating units of compounds. In the plant extract, a few peaks containing impurities appeared as a result of the reaction that took place between silver nitrate and aqueous extract to manufacture silver nanoparticles. Multiple peaks appeared with a measure of 2θ at angles of 14.928°, 30.107°, 38.1°, 43.8°, 64.53°, and 74.14°, where the intensities were different between medium and weak, and corresponded to the XRD measurements of silver nanoparticles (101, 111, 200, 220, and 311).

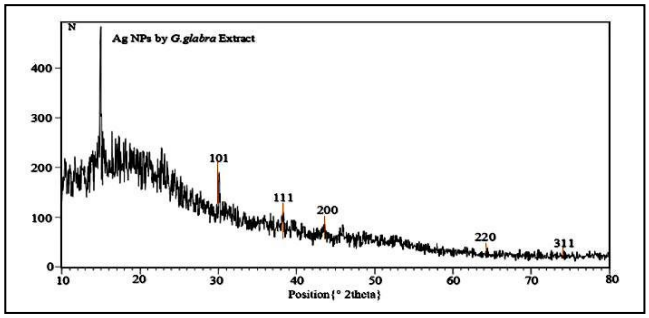

Figure 10. X-ray diffraction of silver nanoparticles biosynthesized from licorice plant extract

The XRD database ICDD, JCPDS file NO: 04-0783 for silver particles confirms the fabrication of silver nanoparticles crystals in this study as they were identical to the XRD database of silver nanoparticles. The results of the current study are in line with those of a study performed by Hamady, Mohammed (24), who reported that silver nanoparticles were also made from different plant sources. In their study, XRD of the manufactured silver nanoparticles was examined and it was identical to the JCPDS database.

Moreover, the findings of this study are consistent with those of a study conducted by Abdullah and Dhahi (25), in which the grape plant was used in the manufacture of silver nanoparticles. In the aforementioned study, the crystal size rate of the silver nanoparticles manufactured from the licorice plant was measured to the peak of 100% using the Debye-Scherrer equations ($D=0.94\lambda/\beta \cos \theta$).

Ultraviolet-Visible Absorption Spectrometer was used to detect the crude aqueous extract of licorice plant and biosynthesized silver nanoparticles at wavelengths of 1100-200 nm. Figure 11 shows the highest absorption peak for the crude extract at a wavelength of 235 nm, which confirms the presence of raw licorice extract as a result of the presence of the glabridin compound since the absorption peaks of this compound appear at the wavelength that is within the range of 350-200 nm. This result is consistent with those of a study conducted by Shanker, Fatima (29), in which the absorption of rays was the ultraviolet of the compound clabridin extracted from licorice powder at the limits of 225.2 and 280.5 nm wavelengths, respectively.

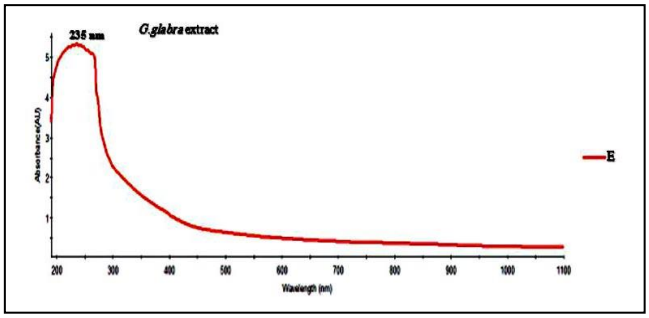

Figure 11. UV-Vis spectrum of the crude aqueous extract of licorice

Figure 12 shows the analysis of ultraviolet rays absorption of biosynthetic silver nanoparticles which confirms the presence of silver nanoparticles. The absorption peak was recorded at the wavelength of 440 nm, and this result was within the diagnostic limits for silver nanoparticles ranging from 400 nm to 450 nm due to surface plasmon absorption. This phenomenon occurs as a result of dipole oscillation, which is formed when the electromagnetic field located within the visible range is combined with the collective oscillation of conduction electrons.

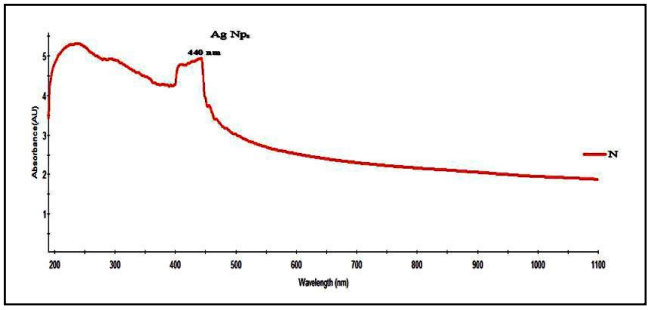

Figure 12. UV-Vis spectrum of the biosynthetic silver nanoparticles extracted from the licorice plant

The phenomenon of plasmon resonance often occurs for metallic surfaces of silver and gold when a beam of light strikes their surfaces. The metallic surface should be angled at a certain angle, and depends on the thickness of the molecular layer of the metal surface; therefore, the size of the formed particles can be counted within the limits of the sizes of nanomaterials according to Alwaan, Jdyea (28). This result was in line with those of a study conducted by Qader, Rashid (15), in which the spectrograph showed ultraviolet visible rays for examination of biosynthesized silver

nanoparticles from Ivy and Aloe Vera extracts with the highest absorption peaks at wavelengths of 419 and 427, respectively.

Results of the current study agreed with those of a study performed by Alwaan, Jdyea (28). In the aforementioned study, the result of examining silver nanoparticles manufactured from extracts of celery and myrtle by ultraviolet-visible spectrometer showed that the highest absorption peak appeared at wavelengths of 408 and 410, respectively. These are within the silver metal absorption limits, which are within the range of 400-450 nm.

To find alternative materials and compounds for chemical drugs that are used as treatments, including cancer diseases, has become an urgent necessity at the present time. In this study, the anti-tumor effects of each of the biosynthesized silver nanoparticles from the licorice plant and its aqueous extract were evaluated on the lung cancer cell line A459. Moreover, its toxicity was determined on the normal fetal liver cell line WRL68 and the differences between them were observed using the MTT assay.

According to figure 13, significant differences appeared (P=0.0129), (P=0.0105) between the effectiveness of the aqueous extract and the biosynthesized silver nanoparticles on A549 lung cancer cells, with a decrease rate of 15.82±1.38 and 4.4±0.76, respectively, at the concentration of 25 µg/ml. There were also significant differences at the concentration of 400 µg/ml between the manufactured silver nanoparticles and the aqueous extract, with inhibition rates of 58.18±3.31 and 49.79±1.99, respectively. In addition, no significant differences were observed between the values of cell growth inhibition at the concentrations of 50, 100, and 200 µg/ml.

The data summarized in table 1 showed that nanoparticles had greater anti-tumor activity, compared to the extract on cancer cells as the inhibitory concentration for half of the cells used in the experiment (IC_{50}) reached 58.78 µg/ml for nanoparticles and 67.44 µg/ml for the aqueous extract. It is worth noting that the lower the IC_{50} inhibitor, the higher the anti-tumor activity. Regarding the toxicity of each of the nanoparticles and the extract on the normal hepatic fetal cell line WRL68 (Figure 14), significant differences were observed between the nanoparticles and the aqueous extract at a concentration of 400 µg/ml, where it reached (P=0.0010) with a vitality rate of 80.75±1.62 and 69.83±2.84, respectively. Moreover, no significant differences were observed at concentrations of 25, 50, 100, and 200 µg/ml, and a comparison between nanoparticles and the aqueous extract (Table 2) proved that the toxicity of the biosynthesized nanoparticles is less than the toxicity of the aqueous extract on normal cells. The IC_{50} values of nanoparticles and aqueous extract were 244.2 µg/ml and 147.0 µg/ml, respectively.

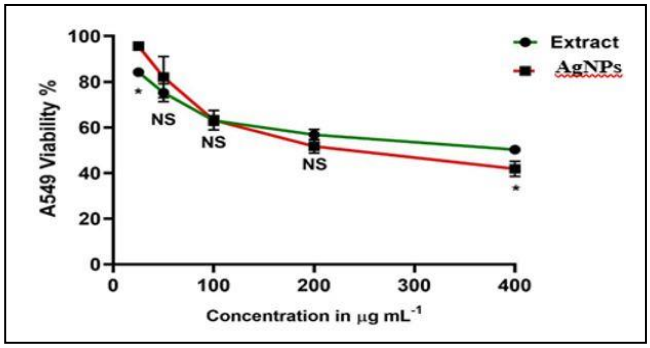

Figure 13. Cell viability (average ± standard deviation) of lung cancer cells A549 after treatment with silver nanoparticles manufactured from licorice and its aqueous extract using *in vitro* MTT assay at 37, 5% carbon dioxide for 24 hours. *: p=0.05, NS: Non-significant, (SD: standard deviation, replicates = 3)

Table 1. A comparison of the anitumor activity between biosynthesized silver nanoparticles and licorice aqueous extract on human lung cancer cell line (A549)

(*P*-Value)	Significancy	Percentage of inhibition rate of lung cancer cells A459 after treatment with SD ± % aqueous extract	Percentage of inhibition rate of A459 lung cancer cells after treatment SD ± % with silver nanoparticles	Conc. µg mL^{-1}
0.0129	*	1.38±15.82	0.76±4.4	25
0.2365	NS	3.95±24.79	9.00±17.94	50
> 0.9999	NS	2.12±39.92	4.30±36.84	100
0.5319	NS	2.36±43.25	2.99±48.34	200
0.0105	*	1.99±49.79	3.31±58.18	400
		IC50: 67.44	IC50: 58.78	

* NS: Non-significant, SD: standard deviation, alpha *P*-value = 0.05

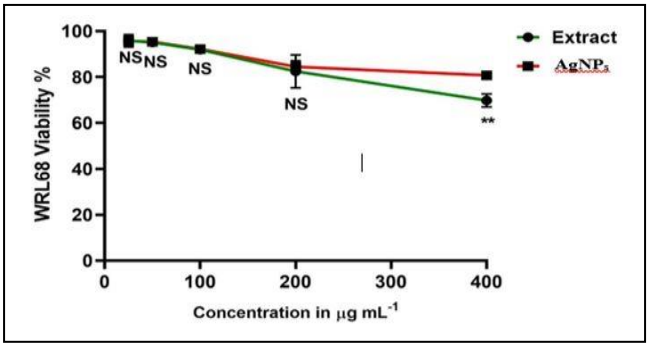

Figure 14. The cell viability (average ± standard deviation) of A549 lung cancer cells after treatment with biosynthesized silver nanoparticles licorice aqueous extract using *in vitro* MTT assay at 37 ℃, 5% carbon dioxide for 24 hours. *: *P*>0.05, NS: Non-significant, SD: standard deviation, replicates = 3)

Table 2. The toxicity of biosynthetic silver nanoparticles compared with licorice aqueous extract on the viability of human normal fetal liver cell line (WRL68)

(*P*-Value)	Significance	Percentage of normal hepatocytes vitality rate WRL68 after treatment with aqueous extract % ± SD	Percentage of normal hepatocyte viability WRL68 after treatment with silver nanoparticles % ± SD	Conc. µg mL-1
>0.9999	NS	95.83±2.24	95.80± 2.68	25
>0.9999	NS	95.06±0.37	95.33±1.99	50
>0.9999	NS	91.90±1.01	92.21± 0.47	100
0.9316	NS	82.45± 7.22	84.45± 2.60	200
0.0010	**	69.83± 2.84	80.75±1.62	400
		IC50: 147.0	IC50: 244.2	

**NS: Non-significant, SD: standard deviation, alpha *P*-value = 0.05

Goel, Sharma (30) reported that active compounds of the licorice plant were used as an antidote to C6 glioma cancer cell tumor with an IC_{50} of 17.5 µM. Basar, Oridupa (31) used licorice plant roots in the manufacture of anti-tumor of lung cancer cells 549A, compared to the normal human keratinocytes HaCaT cell line. In their study, the toxicity that appeared on the normal keratinocytes cell line was low at the concentration of 250 µg/ml. After 24 h of the experiment, the inhibitory concentration was reached. The IC_{50} of licorice extract against A549 and HaCaT cell lines were 189.1 and 241.9 µg/ml, respectively.

Zhou, Xu (32) demonstrated that the isoflavonoid, one of the licorice compounds, was effective in inducing apoptosis in carcinoma lines. Furthermore, Hsieh, Lin (33) in their *in vivo* study proved that the

compound clabridin (extracted from the roots of the licorice plant) is effective against hepatocellular carcinoma cells. Several *in vitro* studies have indicated the mechanism of action of silver nanoparticles, as they can enter cells by way of endo-cytosis and be localized in the space surrounding the nucleus of the cytoplasm and the endo-lysosomal compartment. Besides, silver particles can enter the mitochondria (the energy houses of cells), disrupt the respiratory chain, and produce free radicals of oxygen (ROS) (antioxidants produced by plants as a metabolic byproduct).

These free radicals interact and cause damage to proteins, fats, and acids as well as the nuclear, membranes, and organelles of cancer cells, which in turn begin to express apoptosis genes (34-36). Where biosynthetic silver nanoparticles from the Chinese varnish tree sumac (*Toxicodendron vernicifluum*) were used as an anti-tumor for human lung cancer (A549), which caused damage to the tumor asfig a result of the formation of free oxygen radicals (ROS) according to the above-mentioned mechanism. In a study conducted by Pathak, Kumar (37), a wild lentil extract plant (*Salvia officinalis*) was used to manufacture silver nanoparticles as an antidote for liver cancer (HepG2) and breast cancer (MCF-7), and it showed high inhibitory activity.

Authors' Contribution

Study concept and design: A. G. O.
Acquisition of data: K. M. T.
Analysis and interpretation of data: G. I. A.
Drafting of the manuscript: A. G. O.
Critical revision of the manuscript for important intellectual content: A. G. O.
Statistical analysis: K. M. T.
Administrative, technical, and material support: K. M. T.

Ethics

Not Applicable.

Conflict of Interest

The authors declare that they have no conflict of interest.

References

1. Horikoshi S, Serpone N. Microwaves in nanoparticle synthesis: fundamentals and applications: John Wiley & Sons; 2013.
2. Chaturvedi S, Dave PN, Shah N. Applications of nano-catalyst in new era. J Saudi Chem Soc. 2012;16(3):307-25.
3. Nida T, Khan MJ. Biogenic nanoparticles: an introduction to what they are and how they are produced. Int J Biotech Bioeng. 2017;3:66-70.
4. Karnani RL, Chowdhary A. Biosynthesis of silver nanoparticle by eco-friendly method. Indian J Nanosci. 2013;1(1):25-31.
5. Gajbhiye M, Kesharwani J, Ingle A, Gade A, Rai M. Fungus-mediated synthesis of silver nanoparticles and their activity against pathogenic fungi in combination with fluconazole. Nanomed: Nanotechnol Biol Med. 2009;5(4):382-6.
6. Prabhu S, Poulose EK. Silver nanoparticles: mechanism of antimicrobial action, synthesis, medical applications, and toxicity effects. Int Nano Lett. 2012;2(1):1-10.
7. Ghosh Chaudhuri R, Paria S. Core/shell nanoparticles: classes, properties, synthesis mechanisms, characterization, and applications. Chem Rev. 2012;112(4):2373-433.
8. Zakir M, Lembang M, Lembang M, editors. Synthesis of silver and gold NPs through reduction method using bioreductor of leaf extract of ketapang (terminalia catappa). International Conference on Advanced Material and Practical Nanotechnology; 2014.
9. Ferlay J, Colombet M, Soerjomataram I, Mathers C, Parkin DM, Piñeros M, et al. Estimating the global cancer incidence and mortality in 2018: GLOBOCAN sources and methods. Int J Cancer Res. 2019;144(8):1941-53.
10. Iraq Mohi. Annual report Iraqi cancer registry. 2015.
11. Freshney I. Application of cell cultures to toxicology. Cell Culture Methods for In Vitro Toxicology. 2001:9-26.
12. Manokari M, Ravindran C, Shekhawat M. Production of zinc oxide nanoparticles using aqueous

extracts of a medicinal plant Micrococca mercurialis (L.) Benth. World Sci News. 2016;30:117-28.
13. Al-Othman M, El-Aziz A, Mohamed AM, Hatamleh A. Green biosynthesis of silver nanoparticles using pomegranate peel and inhibitory effects of the nanoparticles on aflatoxin production. Pak J Bot. 2017;49(2):751-6.
14. Selvi KV, Sivakumar T. Isolation and characterization of silver nanoparticles from Fusarium oxysporum. Int J Curr Microbiol Appl Sci. 2012;1(1):56-62.
15. Qader HF, Rashid IH, Oraibi AG. Detection For Activity of Silver And Zinc Nanoparticles That Synthesized By Leav Extract Of Aloe vera And Epipremnum Against Some Bacteria By Bacteriological And Molecular Methads. Baghdad, Iraq: Al-Iraqia University; 2019.
16. Jemal K, Sandeep B, Pola S. Synthesis, characterization, and evaluation of the antibacterial activity of Allophylus serratus leaf and leaf derived callus extracts mediated silver nanoparticles. J Nanomater. 2017;2017.
17. Bharathidasan R, Panneerselvam A. Biosynthesis and characterization of silver nanoparticles using endophytic fungi Aspergillus concius, Penicillium janthinellum and Phomosis sp. Int J Pharm Sci Res. 2012;3(9):3163.
18. Foster KA, Oster CG, Mayer MM, Avery ML, Audus KL. Characterization of the A549 cell line as a type II pulmonary epithelial cell model for drug metabolism. Exp Cell Res. 1998;243(2):359-66.
19. Giard DJ, Aaronson SA, Todaro GJ, Arnstein P, Kersey JH, Dosik H, et al. In vitro cultivation of human tumors: establishment of cell lines derived from a series of solid tumors. J Natl Cancer Inst. 1973;51(5):1417-23.
20. Elengoe A, Hamdan S. Heat sensitivity between human normal liver (WRL-68) and breast cancer (MCF-7) cell lines. J Biotechnol Lett. 2013;4:45-50.
21. Freshney RI. Culture of animal cells: a manual of basic technique and specialized applications: John Wiley & Sons; 2015.
22. Ahmed SA, Al-Saffar AZ, Neama AFT. Anti-proliferative and Cell Cycle Arrest Potentials of 3-O-acetyl-11-keto-β- Boswellic Acid Against Tumor Cell Lines in vitro. Baghdad, Iraq: ALNahrain University; 2021.
23. Nazari S, Rameshrad M, Hosseinzadeh H. Toxicological effects of Glycyrrhiza glabra (licorice): a review. Phytother Res. 2017;31(11):1635-50.
24. Hamady NM, Mohammed AT, Omer KM. Green synthesis of Silver Nano Particles and study their antibacterial activity: University of Anbar; 2017.
25. Abdullah OI, Dhahi RM. The activity of biosynthesized silver nanoparticales on the inhibition of biofilm formation of bacteria isolated from skin infection. Baghdad, Iraq: Al-Iraqia University; 2020.
26. Mock J, Barbic M, Smith D, Schultz D, Schultz S. Shape effects in plasmon resonance of individual colloidal silver nanoparticles. J Chem Phys. 2002;116(15):6755-9.
27. Siddiqi KS, Husen A, Rao RA. A review on biosynthesis of silver nanoparticles and their biocidal properties. J Nanobiotechnology. 2018;16(1):1-28.
28. Alwaan OI, Jdyea IA, Oraibi AG. Biosynthesizing of silver nanoparticles from Apium graveolens and Myrtus communis plants, detection, characterization and study their effect on genetic variation and growth of Pseudomonas aeruginosa. Baghdad, Iraq: Al-Iraqia University. ; 2021.
29. Shanker K, Fatima A, Negi A, Gupta V, Darokar M, Gupta M, et al. RP-HPLC method for the quantitation of glabridin in Yashti-madhu (Glycyrrhiza glabra). Chromatographia. 2007;65(11):771-4.
30. Goel B, Sharma A, Tripathi N, Bhardwaj N, Sahu B, Kaur G, et al. In-vitro antitumor activity of compounds from Glycyrrhiza glabra against C6 glioma cancer cells: identification of natural lead for further evaluation. Nat Prod Res. 2021;35(23):5489-92.
31. Basar N, Oridupa OA, Ritchie KJ, Nahar L, Osman NMM, Stafford A, et al. Comparative cytotoxicity of Glycyrrhiza glabra roots from different geographical origins against immortal human keratinocyte (HaCaT), lung adenocarcinoma (A549) and liver carcinoma (HepG2) cells. Phytother Res. 2015;29(6):944-8.
32. Zhou R, Xu L, Ye M, Liao M, Du H, Chen H. Formononetin inhibits migration and invasion of MDA-MB-231 and 4T1 breast cancer cells by suppressing MMP-2 and MMP-9 through PI3K/AKT signaling pathways. Horm Metab Res. 2014;46(11):753-60.
33. Hsieh MJ, Lin CW, Yang SF, Chen MK, Chiou HL. G labridin inhibits migration and invasion by transcriptional inhibition of matrix metalloproteinase 9 through modulation of NF-κ B and AP-1 activity in human liver cancer cells. Br J Pharmacol. 2014;171(12):3037-50.
34. Redza-Dutordoir M, Averill-Bates DA. Activation of apoptosis signalling pathways by reactive oxygen species. Biochim Biophys Acta Mol Cell Res. 2016;1863(12):2977-92.

35. Saravanakumar K, Shanmugam S, Varukattu NB, MubarakAli D, Kathiresan K, Wang M-H. Biosynthesis and characterization of copper oxide nanoparticles from indigenous fungi and its effect of photothermolysis on human lung carcinoma. J Photochem Photobiol B. 2019;190:103-9.
36. Yesilot S, Aydin C. Silver nanoparticles; a new hope in cancer therapy? East J Med. 2019;24(1):111-6.
37. Pathak M, Kumar V, Pathak P, Majee R, Ramteke PW, Verma A. Green synthesis of silver nanoparticles using Scindapsus officinalis (Gajpipli): in-vitro cytotoxic activity against HepG-2 & MCF-7 cancer cell lines. 2019.